Controlling the Conformation of Arylamides: Computational Studies of Intramolecular Hydrogen Bonds between Amides and Ethers or Thioethers

Robert J. Doerksen,*[a] Bin Chen,[a, b] Dahui Liu,[c] Gregory N. Tew,[d] William F. DeGrado,*[a, c] and Michael L. Klein*[a]

Abstract: The role of an *ortho*-alkylthioether group in controlling the conformation around the ring–N bonds of *meta*-connected arylamide oligomers is studied. Density functional theory (DFT) geometries of model compounds, including acetanilide, an ether acetanilide, and a thioether acetanilide, and their corresponding diamides, show that for either monoamide or diamide the alkyl side chain of the thioether should be perpendicular to the aryl plane, whereas for the ether monoamide, the alkyl side chain is in the aryl plane. DFT ring–N torsional potentials and constrained geometries of the model compounds demonstrate that carbonyl–S repulsion leads to a high torsional barrier and that intramolecular N–H···S and C–H···O hydrogen bonds and ring–amide conjugation lead to N–H having a preferred orientation in the benzene plane pointing towards S. The N–H bond lengthens and the *ortho*-ring C–H bond shortens in a regular pattern in the approach to the preferred orientation. Calculated IR frequencies for the N–H stretch show a clear red shift between model compounds without and with the thioether side chain.

Keywords: acetanilides · amides · density functional calculations · hydrogen bonds · oligomers

Introduction

In recent years, the design of nonbiological polymers with well-defined secondary and tertiary structures has become an area of active research.[1] A major reason for this interest is that, for the first time, modern methods of solid-phase organic chemistry have allowed the synthesis of homodisperse, sequence-specific oligomers with molecular weights approaching 5000 Dalton. From an organic chemist's perspective, oligomers are large, chemically rich, and—if designed correctly—adopt only a few of the thousands of possible conformations in solution. Further, because they are homogeneous compounds, rather than heterogeneous polymers, their structures can be determined to high resolution by NMR spectroscopy and single-crystal X-ray crystallography. From a protein chemist's perspective, these compounds are also exciting, because they can be designed to have structures and properties approaching those of proteins. Finally, these oligomers have captivated the interest of polymer chemists. Compared to traditional polymers, sequence-specific oligomers are challenging to prepare, relatively small in size, and only available in very limited quantities (milligrams). However, the knowledge and experience gained from these homodisperse oligomers allows us to design "smart" polymers that can perform a certain task, respond to external or internal signals, and so on.

Hydrogen bonds have figured prominently in many strategies for controlling the conformations of designed oligomers. In particular, arylamides have been substituted with alkoxy substituents at the 2-position that form intramolecular hydrogen bonds to the adjacent amide proton (**A**–**C**).[2] Similarly, we have used 2,5-disubstituted aryl thioethers to conformationally restrict the backbone of a series of arylamides (**D**).[3,4]

[a] Dr. R. J. Doerksen, Prof. Dr. B. Chen, Prof. Dr. W. F. DeGrado, Prof. Dr. M. L. Klein
Department of Chemistry, University of Pennsylvania
231 S. 34th St., Philadelphia, PA, 19104–6323 (USA)
Fax: (+1) 215-573-6233/7229/8726
E-mail: rjd@cmm.upenn.edu
wdegrado@mail.med.upenn.edu
klein@lrsm.upenn.edu

[b] Prof. Dr. B. Chen
Present address: Department of Chemistry
Louisiana State University, 232 Choppin Hall
Baton Rouge, LA 70803–1804 (USA)

[c] Dr. D. Liu, Prof. Dr. W. F. DeGrado
Department of Biochemistry and Biophysics
University of Pennsylvania School of Medicine
1010 Stellar Chance Laboratories
Philadelphia, PA 19104–6059 (USA)

[d] Prof. Dr. G. N. Tew
Polymer Science and Engineering Department
120 Governors Dr., University of Massachusetts
Amherst, MA, 01003 (USA)

Supporting information for this article is available on the WWW under http://www.chemeurj.org/ or from the author: methodological details, tables of calculated geometrical parameters, and *xyz* coordinates for **1**–**7** and for 14 conformations of **6**.

© 2004 Wiley-VCH Verlag GmbH & Co. KGaA, Weinheim
DOI: 10.1002/chem.200400176

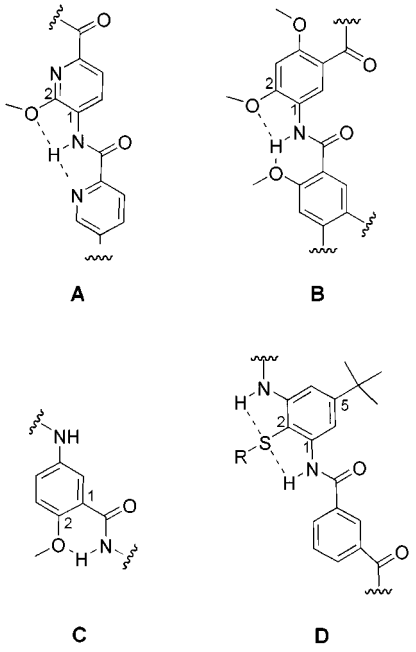

The success of these strategies will depend on the strength of the hydrogen bonds, as well as the overall conformational properties of the amides. The N−H···S hydrogen bond is less well studied than N−H···O. We wished to determine whether such hydrogen bonds would be suitable and strong enough to contribute significantly to the stabilization of particular conformations of oligomers such as **D**. Also, conventional wisdom holds that the alkyl ether or thioether group will lie in plane with the ring, with one pair of electrons in resonance with the ring and the other nonbonding lone pair available for the formation of hydrogen-bonding interactions with the adjacent amide proton. However, it is important to assess the strength of this interaction relative to that in which the alkyl group has rotated out of the plane of the ring. We expected that a second substituent at the 3-position, not present in **A**–**C**, might override this preference (Scheme 1).

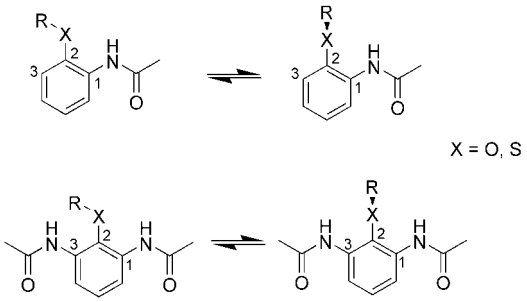

Scheme 1. In-plane versus out-of-plane alkyl group.

The compounds that motivated the current study are a series of oligomers and polymers that were designed[3] to mimic the properties of host defense peptides such as magainin.[5] The monomer unit of **D** was designed to prevent rotation around the backbone ρ [C-C-N-C(O)] and σ [C-C-C(O)-N] angles (cf. **1**, Scheme 2). Here we examine in detail how the thioether side chain helps to control the conformation around each ring–N torsional angle ρ. Additionally, we examine the torsional potential associated with τ for the ring–S connection. In future work we will examine the conformation around σ, which also is important for the extended structure of **D**.[6]

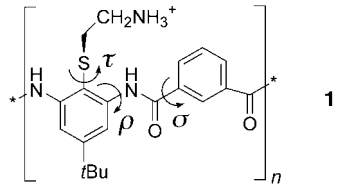

Scheme 2. Key torsional angles in **1**.

We consider the conformation of model compounds related to **A**–**D** using a variety of computational approaches. We present calculated lowest energy structures for **2**–**7**. These

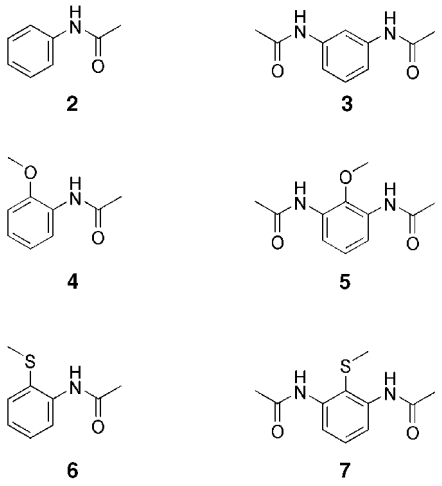

compounds allow a comparison of unsubstituted acetanilide (*N*-acetylaniline, **2**) with the corresponding ether (**4**) and thioether (**6**), and of each of these three monoamides with its corresponding diamide (**3**, **5**, and **7**). For **2** and **6**, we calculated C-C-N-C torsional potentials and N−H stretch vibrational frequencies in order to compare further the influence of the thioether on the conformation of **D**. Experimental IR vibrational frequency shifts are regularly used to characterize intramolecular hydrogen bonding.[7]

Results and Discussion

Structure of lowest energy conformations: The optimized structures for model compounds **2**–**7** are shown in Figure 1. For all molecules, each amide group is coplanar with the benzene ring. Two orientations ($\rho = 0$ or 180°) of each amide in **3** are possible, but we examined only the conformer in which both amides have $\rho = 0°$, pictured in Figure 1.

 © 2004 Wiley-VCH Verlag GmbH & Co. KGaA, Weinheim

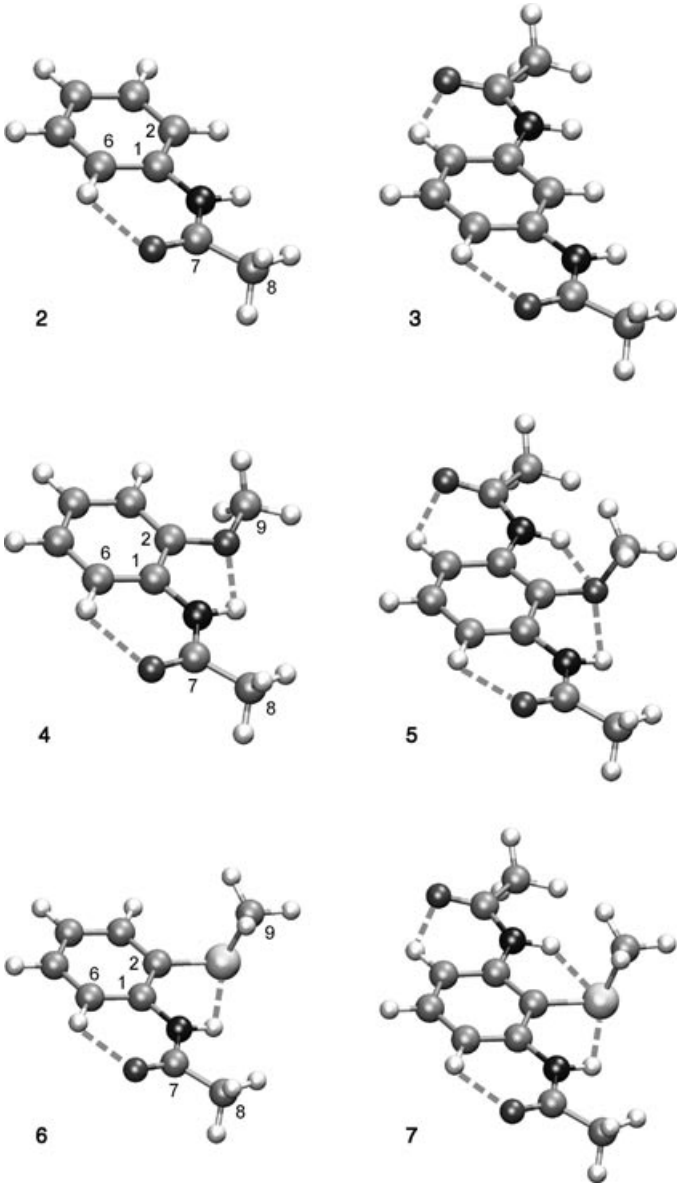

Figure 1. B3LYP/6-311G(d,p) optimized minimum structures for unsubstituted arylamides **2** and **3**, ethers **4** and **5**, and thioethers **6** and **7**. The amide groups are all in the benzene plane. See text for details. Carbon atom numbering is shown for **2**, **4**, and **6**. From light to dark, the atom types are H, S, C, O, and N. Hydrogen bonds are shown as dashed lines.

Comparison of monosubstituted ether and thioether: The lowest energy conformation for **4** (which contains only one amide side group) has the *O*-methyl group in the plane of the benzene ring, although the optimization was begun with the methoxyl group perpendicular to that plane. By contrast, the methylthio group forms a right angle to the aryl plane, even in **6**, which has only one amide side group. To determine the basis for this change, we examined the N−H···X hydrogen-bond geometric parameters for **4** and **6**, calculated with BLYP or B3LYP and two different basis sets (Table S1, Supporting Information). Using B3LYP and a larger basis set changes the geometric parameters, for example, reducing N···S in **6** by 0.027 Å, but does not significantly change the differences between **4** and **6** for the listed geometric parameters. Hence, the results seem well-converged with improving method. The geometry of acetanilide (**2**) has been obtained by neutron diffraction at several temperatures[8] and calculated by Hartree–Fock/6-31G*.[9] Our calculated geometry agrees very well with those results. The discussion below is only for parameters from the most accurate, B3LYP/6-311G(d,p) calculations.

Further comparison of unsubstituted acetanilide to the ether and thioether derivatives reveals some major differences (Table 1). Perhaps the most important difference is that the C-C-X angles are close to 120° in all cases except for ether **4**, which has C-C-O angles of 114.6 and 124.4° (Scheme 3). The O atom of **4** is pushed towards the amide N−H group to minimize steric repulsion between its in-plane methyl group and the neighboring aryl H atom. Because of this, the nonbonded distance (N)H···X is shortest for **4** (2.112 Å) and significantly longer in **2** and **6**. Another noteworthy difference, but one that illustrates a generally observed contrast between O and S, is that the C-O-C angle is 118.6° in **4**, but the C-S-C angle is just 100.8° in **6**.

The geometrical parameters can help in assessing the relative hydrogen-bond strength in ether **4** versus thioether **6**. Of course, C−X and X−C depend strongly on X, with C−O bond lengths of 1.374 and 1.421 Å for **4**, and C−S bond lengths of 1.799 and 1.839 Å for **6**. Because of this typical difference in carbon–heteroatom bond lengths, the N−H···X angles also differ in a regular pattern. The N−H···O angle of 108.3° for the ether compares to a N−H···S angle of 116.6° for the thioether. This helps make the thioether the more suitable for hydrogen bonding: the resulting five-membered hydrogen-bonded ring has a better shape in the thioether, since a wider angle (closer to linear) is usually more suitable for hydrogen bonding. Compared to acetanilide (**2**), the methoxyl group induces a small change in the N−H bond length, whereas the methylthio group increases it by about 0.005 Å, also suggestive of stronger hydrogen bonding for the thioether. The six-membered hydrogen-bonded

Table 1. Calculated[a] N−H···X [X = H, O(CH_3), S(CH_3)] hydrogen bond geometric parameters[b,c] for **2**–**7**, which contain one or two $NHCOCH_3$ side chains *ortho* to X.

Molecule	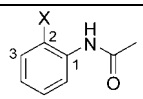			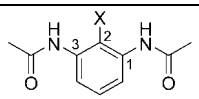		
Parameter	X = H **2**	X = OCH_3 **4**	X = SCH_3 **6**	X = H **3**	X = OCH_3 **5**	X = SCH_3 **7**
N−H[b]	1.008	1.009	1.013	1.008	1.009	1.012
N···X[b]	2.606	2.611	3.021	2.593	2.704	2.990
H···X[b]	2.256	2.112	2.426	2.246	2.229	2.400
N−H···X[c]	98.6	108.3	116.6	98.5	107.1	116.4
C2-X[b]	1.086	1.374	1.799	1.087	1.394	1.799
C2-X-Me[c]	–	118.6	100.8	–	113.6	101.0
C1-C2-X[c]	119.7	114.8	121.0	119.4	119.2	120.0
C3-C2-X[c]	119.8	124.8	119.2	119.4	119.2	120.0

[a] B3LYP/6-311G(d,p). [b] Distances in Ångstroms. [c] Angles in degrees.

© 2004 Wiley-VCH Verlag GmbH & Co. KGaA, Weinheim

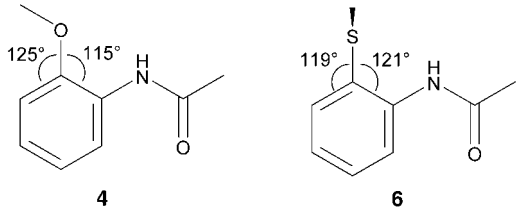

Scheme 3. A comparison of external angles for ether **4** and thioether **6**.

OCNCCH ring is very similar for all the model compounds. In all three monoamides, C3–H, which is the C–H group involved in the C–H···O hydrogen bond, has a length of 1.079 Å, significantly shorter than the 1.084 Å of C4–H. This matches the neutron diffraction geometry of **2**.[8]

Disubstituted versus monosubstituted ethers and thioethers: Comparing the B3LYP/6-311G(d,p) geometries of **2–7** (Table 1), with one or two amide side chains, leads to the same geometric parameters in most cases. The main differences are found for the ethers, since monoamide **4** is the only case in which the side chain methyl group is in the plane of the benzene ring. This leads to several effects: the C–O single bonds are about 0.02 Å shorter in monoamide **4** than in diamide **5**; the two C-C-O angles are 114.8 and 124.8° for **4**, but both 119.2° for **5**; and C-O-C is 118.6° for **4** but 113.6° for **5**. Thus there is more sp^2 character for the O atom of **4** compared to that of **5**. This was also reflected in a shorter (by 0.117 Å) (N)H···O distance in the monoamide ether versus the diamide ether. This shortening was not observed in the unsubstituted amides (**2** vs **3**) or the thioether amides (**6** vs **7**), which instead showed a slight lengthening. Other differences between the monosubstituted and disubstituted compounds are small. Therefore, in the calculation of torsional potentials to consider the effects of the thioether on arylamide torsion below we chose to use **2** and **6**, rather than the larger but more computationally demanding **3** and **7**.

Energy landscape of thioether 6: To ensure that the structure of **6**, shown in Figure 1, represents the minimum energy conformer, we calculated the geometry of 14 different conformations of **6** using the CPMD program and the HCTH density functional (see Computational Methods and Supporting Information). The initial dihedral angles (see Figure 2) and relative energies of these structures are listed in Table 2. The final dihedral angles did not vary much from the initial ones.

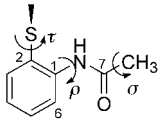

Figure 2. 2-Methylthioacetanilide (**6**), with ρ torsional angle in the 0° conformation and $\tau = 90°$; $\sigma = 0°$ means that a methyl H atom is coplanar with and *syn* to the carbonyl O atom. Numbering of carbon atoms is shown.

Table 2. CPMD/HCTH approximate dihedral angles[a] and relative stabilities[b] of various conformations of **6**, calculated with two different box sizes.

Approximate dihedral angles[a]			ΔE[b]	
τ[c]	ρ[d]	σ[e]	A[f]	B[g]
90	0	0	0.2	
90	0	180	0.0	0.0
90	90	0	6.8	
90	90	180	6.5	6.5
90	180	0	15.1	14.9
90	180	180	15.0	
90	270	0	8.5	
90	270	180	8.3	8.7
180	0	0	2.0	1.9
180	0	180	1.8	1.7
180	90	0	5.1	
180	90	180	4.9	
180	180	0	12.1	
180	180	180	12.2	

[a] In degrees. [b] In kcal mol^{-1}. [c] C1-C2-S-C9. [d] C6-C1-N-C7. [e] O-C7-C8-H. [f] Box size: 10×14×14 Å. [g] Box size: 10×12×12 Å.

Table 2 shows that the lowest energy conformation of **6** has the methyl group on the S atom perpendicular to the plane of the benzene ring ($\tau \approx 90°$), the N–H group directed towards S ($\rho \approx 0°$), and a methyl H atom directed *anti* to the carbonyl O atom ($\sigma \approx 180°$). The least stable conformation listed, which has the carbonyl group directed toward the S atom, is about 15 kcal mol^{-1} above the lowest energy structure. Restricting the methylthio group to be coplanar with the benzene plane ($\rho \approx 180°$) decreases the stability of the lowest energy conformation by 1.8 kcal mol^{-1}. However, for structures having $\rho \neq 0°$, the structures with $\tau = 180°$ are more stable, since repulsive contacts are avoided between the carbonyl and methylthio H atoms (for $\rho = 270°$) or between the amide N–H group and methylthio H atoms (for $\rho = 90°$). Placing a methyl H atom *syn* to the carbonyl O atom ($\sigma \approx 0°$) generally leads to a structure less stable by about 0.2 kcal mol^{-1}. This is similar to the barrier found for the methyl torsion of acetanilide recently determined by ZEKE spectroscopy to be between 0.29 and 0.86 kcal mol^{-1},[10] and by millimeter-wave absorption spectroscopy to be 0.14 kcal mol^{-1}.[11] Considering only $\sigma = 180°$ structures, for $\rho = 0°$, changing τ from 90 to 180° makes **6** less stable by 1.8 kcal mol^{-1}. For $\rho = 90°$, $\tau = 180°$ is more stable than $\tau = 90°$ by 1.6 kcal mol^{-1}. This suggests that having $\rho = 0°$ stabilizes the $\tau = 90°$ structure versus the $\tau = 180°$ structure by 3.4 kcal mol^{-1}, most probably because of steric repulsion between the H atom of N–H and the methyl H atoms.

Table 2 also lists relative energies calculated for structures placed in a slightly smaller 10×12×12 Å box. The relative energies agree with those from the calculations with the larger box, with an absolute average difference of only 0.24 kcal mol^{-1}. For three of the structures, we also used a 12×14×14 Å box. Again the relative energies were similar. This suggested that it would be accurate enough to use the 10×12×12 Å box for calculating the torsional potentials of **6**.

It is important also to assess the size of possible errors caused by the choice of method. Relative energies at the

 © 2004 Wiley-VCH Verlag GmbH & Co. KGaA, Weinheim

CPMD/HCTH geometries for five conformations of **6** were also calculated by Hartree-Fock (HF) and second-order Møller–Plesset perturbation theory (MP2) with two basis sets (Table 3). The inclusion of diffuse functions in the basis set [6-31++G(d,p)] does not change the HF results significantly, but changes the MP2 results by as much as 1.9 kcal mol^{-1}. This is typical in that it is easier to reach the basis set limit for HF than for MP2. With the larger 6-31++G(d,p) basis set, HF and MP2 agree very well, except that HF overestimates the $\rho = 180°$ barrier by 2.1 kcal mol^{-1}. Comparison with the density-functional HCTH/70 Ry results shows most importantly that all methods agree on which structure is of lowest energy. The HCTH barrier height for 180° torsion around ρ agrees perfectly with MP2. However, the differences between HCTH and MP2 for the other three points in Table 3 are as large as 3.9 kcal mol^{-1}. Note that the HF and MP2 relative energies were calculated without optimizing the geometry at that level, in order to save computational time. With MP2/6-31G(d), optimizing the geometry of the $\rho = 0°$, $\tau = 90°$ structure led to a structure lower in energy by 0.8 kcal mol^{-1}. Differences could be greater for the other conformations. This suggests that it would be worthwhile in subsequent studies to verify further the accuracy of DFT and of the particular functional and cutoff used here with tests including optimizing the geometry and using better basis sets and higher-order treatments of electron correlation.

Table 3. Comparison of CPMD/HCTH with HF and MP2 with two different basis sets (all at the CPMD/HCTH geometries) for relative stabilities of conformations of **6**.

Approximate dihedral angles[a]		ΔE[b]				
τ[c]	ρ[d]	HCTH[e]	HF[f]	HF[g]	MP2[f]	MP2[g]
90	0	0	0	0	0	0
180	0	1.8	4.1	3.9	3.7	4.0
90	90	6.5	3.2	2.9	4.0	2.6
90	270	8.3	5.7	5.2	7.0	5.1
90	180	15.0	16.8	17.1	15.1	15.0

[a] In degrees; σ = O-C7-C8-H = 180° for all cases. [b] In kcal mol^{-1}. [c] C1-C2-S-C9. [d] C6-C1-N-C7. [e] With a 70 Ry cutoff in a box of dimensions 10 × 14 × 14 Å. [f] With 6-31G(d,p) basis set. [g] With 6-31++G(d,p) basis set.

C-C-N-C torsional potentials:

*C-C-N-C torsional potentials of acetanilide (**2**) and thioether **6***: Next consider torsional potentials for the torsional angle ρ (C-C-N-C), around the bond connecting the benzene ring and the N atom of the amide unit. Figure 3 shows ρ plots for **2** and **6**. Each point on the graph represents a structure in which ρ was constrained but all other geometric parameters were optimized (using CPMD/HCTH; see Computational Methods). As the constrained angle ρ is varied, all other geometrical parameters are free to change, and indeed they do so greatly, often in regular patterns; details will be published elsewhere.[6] However, some of the changes relevant to hydrogen bonding are discussed below. Several of the constrained structures are also depicted in Figure 3.

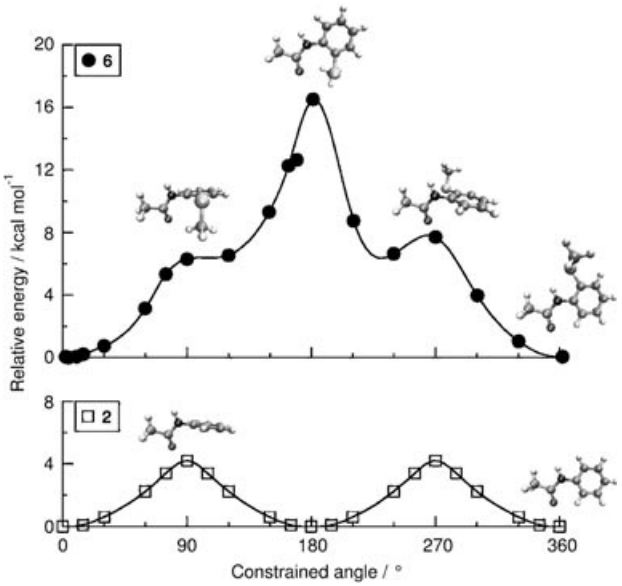

Figure 3. CPMD/HCTH relative energies [kcal mol^{-1}] for geometries with constrained ring–amide C-C-N-C torsion angle ρ for **6** and **2**. Some of the constrained structures are shown: the ca. 0° (shown at ca. 360°) and ca. 90° conformations for each compound, plus the approximately 180° and approximately 270° conformations for **6**. For clarity, all the structures are drawn with the amide group in the same orientation. The curves are spline fits to the data points. Atom coloring as in Figure 1.

The methylthio side chain creates profound changes in the torsional potential, because of the attraction of the N–H···S hydrogen bond (from roughly −60 to +60°, Figure 3) and the repulsion between the carbonyl group and S atom (from 120 to 240°). Also, the potential is no longer symmetric about 180°, since near 90° the carbonyl group is *syn* to the methylthio group and a stabilizing (C)H···O interaction with the nearest methylthio H atom becomes possible.

The various factors which modify the ρ torsional potential of **6** compared to **2** confirm that the carbonyl group should always point away from the thio-linked side chain. The peaks at $\rho = 90$ and 270° are much higher for thioether amide **6** than for **2**. Based on the difference, we calculate that the methylthio group raises the 0–90° barrier in **6** versus **2** by about 2 kcal mol^{-1} and the 360–270° barrier by about 3.4 kcal mol^{-1}. The difference between those two of about 1.4 kcal mol^{-1} can be partially attributed to the role of the O···H(CS) bond.

Recently François et al.[12] described the effects of N–H···S hydrogen bonds on the stability of an Fe^{III} complex. They found that six N–H···S hydrogen bonds stabilized the complex by about 10 kcal mol^{-1} relative to a suitable control; this suggested the strength of each N–H···S hydrogen bond to be about 1.7 kcal mol^{-1}. This is similar to the estimate of 2 kcal mol^{-1} in this work. Also it was found that the S-containing hydrogen bonds helped stabilize the complex better than N–H···O hydrogen bonds.[12]

*C-C-N-C torsional potentials of acetanilide (**2**) versus benzanilide*: Since the target oligomer structure **1** has another benzene ring attached after the carbonyl group, we also calculated the ρ torsional potential for benzanilide, which is

© 2004 Wiley-VCH Verlag GmbH & Co. KGaA, Weinheim

the same as **2** except that the carbonyl methyl group is replaced by a benzene ring.[6] The barrier height and curve shape for rotation around ρ are very similar in **2** and benzanilide.[6] Thus, the group attached to the carbonyl end of the amide makes little difference to the ring–N torsional potential. This supports our use of the more compact methyl, rather than phenyl, amide end group when considering the effects of including an *ortho*-methylthio group.

Vibrational frequencies: Previous published work has shown that when there is an N–H···S hydrogen bond, the N–H stretch IR frequency ω can be red-shifted by as much as 161 cm^{-1} to a final value of about 3228–3281 cm^{-1}.[13] By contrast, for N–H adjacent to S of a disulfide there was no noticeable shift, and the authors concluded that there was no hydrogen bonding in that case.[14] Calculated BLYP/6-31G(d,p) IR frequencies and intensities *I* for the amide N–H stretch in **2**–**7** are listed in Table 4. The frequency ω is red-shifted by 84–104 cm^{-1} when the *ortho* side group X is changed from H to SCH_3. By contrast, changing from H to OCH_3 shifts ω by a much smaller amount and even increases the frequency in **4**. Also, Table 4 shows that the IR intensities increase much more in **6** and **7** than in **4** and **5**, compared to **2** and **3**. These effects match what was found above for the changes in N–H bond length, that is, it is significantly longer only for the thioethers, not for the ethers.

Table 4. Calculated BLYP/6-31G(d,p) harmonic N–H vibrational frequencies[a] (ω) and intensities[b] (*I*) for **2**–**7**.

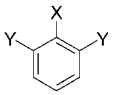

	No. of Y[d]	X = H	X = OCH_3[f]	X = SCH_3[g]	Δ[c] OCH_3[f]	Δ[c] SCH_3[g]
ω	1	3510	3515	3406	5	−104
	2[h]	3513	3497	3425	−16	−88
	2[i]	3513	3498	3430	−15	−84
I	1	9	36	86	28	77
	2[h]	8	20	71	12	63
	2[i]	8	36	62	28	54

[a] In cm^{-1}. [b] In km mol^{-1}. [c] Difference with respect to X = H. [d] Number of $NHCOCH_3$ groups. [e] **2** and **3**. [f] **4** and **5**. [g] **6** and **7**. [h] Asymmetric stretch. [i] Symmetric stretch.

Table 5 lists results for **2** and **6** calculated with other methods. The B3LYP ω are larger than the BLYP ones using the same basis set. Improving the basis set reduces the frequencies slightly. Using a scaling factor of 0.97 for B3LYP/6-311G(d,p)—previous recommendations were 0.9614 for B3LYP/6-31G(d)[15] and 0.9762 for B3LYP-Sadlej[16]—yields a difference in ω of 89 cm^{-1}. The intensity increases from 18 to 88 km mol^{-1}. Each change is similar to but smaller than the effect found for BLYP/6-31G(d,p). In previous work,[17] harmonic frequencies calculated with the HCTH functional and plane wave basis set,[17] also scaled by 0.97, gave a larger difference in ω between **6** and **2** than the B3LYP results. The most accurate calculated results should be the HCTH frequencies from Car–Parrinello dynamic simulations, which include anharmonic effects. Several simulation procedures gave similar results.[17] These are considerably lower than the harmonic ones, but also predict the red shift, 78 cm^{-1}, to be close to that given by the scaled B3LYP/6-311G(d,p) results. Thus, calculated IR data from several methods agree with previously published experimental IR data and show that there is a significant interaction between the methylthio group and the amide N–H group pointing to it.

Table 5. Calculated harmonic and experimental N–H vibrational frequencies[a] (ω) and intensities[b] (*I*) with and without methylthio side chain.

	Method[c]		**2**	**6**	Δ[d]
ω	BLYP	6-31G(d,p)	3510	3406	−104
	B3LYP	6-31G(d,p)	3636	3544	−91
	B3LYP	6-311G(d,p)	3627	3535	−92
	B3LYP[e]	6-311G(d,p)	3518	3429	−89
	HCTH[e,f,g]	90 Ry[h]	3490	3369	−121
	HCTH[g,i]	90 Ry[h]	3309	3231	−78
I	BLYP	6-31G(d,p)	9	86	77
	B3LYP	6-31G(d,p)	16	84	68
	B3LYP	6-311G(d,p)	18	88	69

[a] In cm^{-1}. [b] In km mol^{-1}. [c] See text for details. [d] Difference between **2** and **6**. [e] Scaled by 0.97. [f] Calculated by finite difference at optimized geometry. [g] From ref. [17]. [h] Energy cutoff for plane wave basis set. [i] From a multipicosecond Car–Parrinello molecular dynamics simulation controlled by Nosé–Hoover chains of frequency 3200 cm^{-1}, with $T \approx 300 \pm 50$ K.

N–H···S hydrogen bonds: Weak N–H···S hydrogen bonds[18,19] have been identified in many X-ray[13,14,20] and neutron diffraction studies. In one particularly relevant example, Rahman and van der Helm[20a] studied the X-ray crystal structure of *N,N′*-diacetyl-3-methylthiobenzidine, a biphenyl derivative in which one ring is the same as **2** and the other as **6**. They found the methyl group on the S atom to be perpendicular to the benzene plane, the amide group adjacent to it to be rotated by about 12° out of the plane but with the N–H group pointing toward the S atom, and the amide on the other ring to be rotated out of its neighboring benzene plane by about 60°. However, the crystal structure includes extensive intermolecular hydrogen bonding, which makes it hard to assess the impact of intramolecular N–H···S bonds.[20a]

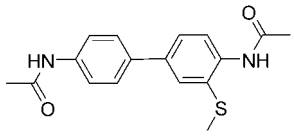

N,N-diacetyl-3-methylthiobenzidine

In a systematic review of X-ray crystal structures, Allen et al.[20b] studied the ability of divalent S to form hydrogen bonds. They found 115 cases of intramolecular N–H···S hydrogen bonding (carefully excluding H···S 1,3 and 1,4 interactions; see Table 6). The mean geometrical parameters for

 © 2004 Wiley-VCH Verlag GmbH & Co. KGaA, Weinheim

Table 6. Intra- and intermolecular N–H···S geometrical parameters[a] from experiment and this work.

Source	Cases	N–H	H···S	N···S	N–H···S
neutron[b,c,d]	8	1.020(4)	2.48(6)	3.44(4)	–[e]
neutron[b,d,f]	1	1.041(2)	2.274(2)	3.287(2)	–[e]
X-ray[c,d,g]	26	–[e]	2.74(2)	3.58(3)	145(3)
X-ray[d,g,h]	115	–[e]	2.60(2)	3.12(2)	113(1)
X-ray[d,h,i]	2	0.860	2.497	2.978	116.1
6[h,j,k]	1	1.013	2.426	3.019	116.6
7[d,h,j,k]	2	1.012	2.400	2.990	116.4

[a] Lengths in Ångstroms; angles in degrees. [b] Ref. [20c]. [c] Intermolecular. [d] Mean. [e] Not given in source. [f] Shortest. [g] Ref. [20b]. [h] Intramolecular. [i] Ref. [3]. [j] This work. [k] B3LYP/6-311G(d,p).

H···S and N···S were 2.60 and 3.12 Å, respectively, and for N–H···S it was 113°. Note that in the work of Nakamura et al.[13,14] on X-ray structures of arylamide–S/transition-metal complexes that are stabilized by one or two N–H···S interactions, the N···S distances ranged from 2.89 to 3.02 Å.

Steiner[20c] considered eight reported cases of N–H···S hydrogen bonds from neutron diffraction, which can more accurately determine the position of the H atoms than X-ray diffraction. The mean geometrical parameters for N–H, H···S, and N···S were 1.020, 2.48, and 3.44 Å, respectively. Comparing Steiner's work to that of Allen et al. reveals that the X-ray N···S mean distance is much shorter than that from neutron diffraction. This is probably because Steiner's study included intermolecular hydrogen bonds, which tend to be more linear and thus can be longer. Indeed, in reference [20b] the mean intermolecular N···S distance is much longer than the mean intramolecular one. Steiner noted a trend that shorter H···S distance is correlated with longer N–H distance in those structures. The longest N–H bond, 1.041 Å, is matched with the shortest H···S distance of 2.274 Å.

For **6**, Figure 4 shows the most notable X–H bond length changes, for N–H and C6–H, with respect to those found in the quasiplanar 181.4° structure. The N–H bond is stretched by 0.008 Å in the lowest energy conformation (when the N–H group is pointed most directly toward S); by comparison, in **2**, the N–H bond length varies only over a range of 0.0003 Å for a torsion of $\rho = 0$–90°. The elongation of the N–H bond when it is directed toward the S atom suggests the occurrence of an N–H···S hydrogen bond. The calculated H···S and N···S lengths and N–H···S angles of **6** and **7** also are close to the average values found from the experimental surveys.

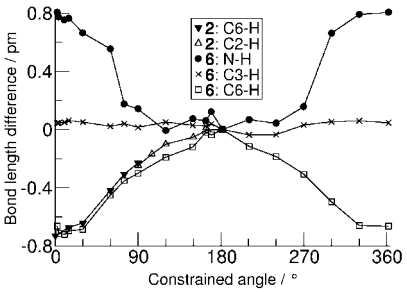

Figure 4. Bond length differences for X–H bonds (X = N, C) for various structures with constrained ρ. For **2**, the data is adjusted from structures with $\rho = 0$–90° (for C2–H or C6–H), by taking the difference from C6–H for $\rho = 0°$. For **6**, the differences are relative to the $\rho \approx 180°$ structure. Carbon atom numbering as in Figure 1.

The X-ray structure from our previous work[3] (average of two N–H···S cases in a molecule the same as **8**, except for a different end group on the SR side chain), is close to that calculated in this work for **6** and **7** for N–S and N–H···S (Table 6); the agreement is not as good for N–H and H···S, primarily due to the overall quality of the crystal and the difficulty in locating hydrogen atoms in X-ray structures. The calculated N–H···S hydrogen bond parameters in **6** and **7** match Steiner's description[18] of a weak hydrogen bond.

C–H···O hydrogen bonds: Weak C–H···O hydrogen bonds have received much attention in recent years.[18,21,22] Several older studies[23] already had provided insight into the way such interactions influence the conformation of a molecule or complex. There is an increasingly clear understanding that C–H bonds usually shorten when participating in a hydrogen bond, as found in this work. Gu et al.[21] point out that in hydrogen bonds there is a balance between various forces, and suggest that when a C–H bond is involved in a C–H···O interaction, it is shortened because the electrostatic, charge transfer, polarization, and dispersion forces which pull the H atom away from the C atom, lengthening the bond, have a smaller effect than the exchange forces, which shorten the C–H bond by pushing the hydrogen atom away from the acceptor.

In unsubstituted **2**, as ρ is changed from 0° to 90° (note, for $\rho = 0°$, N–H is pointing toward C2, and C=O toward C6, see Figure 1), the C6–H bond stretches by 0.005 Å and is shortest when the carbonyl group points toward it ($\rho = 0°$). The effects of C–H···O hydrogen bonding were noted already in the neutron diffraction study on **2**.[8,9] By contrast, the C2–H bond varies over a range of only 0.0023 Å, and the N–H bond over 0.0003 Å.[24] In thioether **6**, the C6–H bond also is shortest when it is involved in a C–H···O hydrogen bond in the $\rho = 0°$ structure. In **6**, as ρ is varied from 0–90°, the C6–H bond lengthens by 0.004 Å, in a way that Figure 4 shows is very similar to **2**. Thus the typical behavior of a weak C–H···O hydrogen-bonding interaction is followed in **2** and **6**. Note that though C–H···O interactions are important for the lowest energy structures of all the model compounds in this work, they provide no special stability to **6** compared to the other structures.

Conclusion

Our results from model compounds show that in the target arylamide polymers **D**, adding the *ortho* thioether group helps keep the amide group in the plane of the benzene ring, with the N–H group pointing towards S and the C=O group *anti* to the S atom. For the acetanilides, the ether group was in-plane whereas the thioether group was out of the aryl plane. For the corresponding diamides, ether and thioether groups should each be out of plane. Density functional theory C-C-N-C torsional potentials and constrained geometries showed a high, repulsive barrier for C=O point-

© 2004 Wiley-VCH Verlag GmbH & Co. KGaA, Weinheim

ing toward S and that the N–H bond stretches in a regular pattern as it is rotated to point towards the S atom. There is good evidence for a weak N–H···S hydrogen bond in **6**: the N–H bond stretches by 0.008 Å when pointed toward S; the C-C-N-C 0–90° barrier height is increased in **6** versus **2** by 2 kcal mol^{-1}; the N–H stretching frequency is red-shifted and has higher intensity in **6** versus **2**. Previous work has also shown that the N–H group points towards S in an X-ray crystal structure,[3] tends to point towards S in MD[3] and CPMD simulations,[17] and that the methylthio group helps to restrict rotation around the ring–N bond.[17] From the IR frequency shifts and structures of model species **2–7**, it seems that hydrogen bonding is much clearer in the thioethers than in the ethers, possibly because the N–H···X dimensions for the thioether are more suitable for hydrogen bonding than those of either the monoamide or diamide ether.

Computational Methods

Gaussian 98[25] was used to obtain geometries for **2–7** by using DFT[26] with the gradient-corrected BLYP[27] functional and the standard 6-31G(d,p) basis set, and the hybrid B3LYP[27b,28] functional with 6-31G(d,p) and the valence triple-zeta plus polarization 6-311G(d,p) basis sets.[29] Harmonic vibrational frequencies were calculated to ensure that each stationary point reached was a minimum.

To tackle the large number of different possible conformations of **6**, we used the Car–Parrinello Molecular Dynamics (CPMD) program,[30] which is well-parallelized to run on many processors, to get fast and reasonably accurate results. Reference [31] provides an excellent overview of the CPMD method and program. In all CPMD calculations in this work the HCTH[32] density functional was used, which gives more accurate relative energies than BLYP or B3LYP for standard training set cases.[32] In the CPMD program, a plane wave basis set is used, which is expanded to a certain energy cutoff; here we used 70 Ry unless mentioned otherwise. Core electrons were described with Trouiller–Martins norm-conserving pseudopotentials[33] (optimized for the HCTH functional) by using the Kleinman–Bylander integration scheme.[34]

Single-point energy calculations were performed at the CPMD/HCTH geometries of some of the different conformations of **6** with Gaussian 98,[25] using Hartree–Fock (HF) and second-order Møller–Plesset perturbation theory (MP2), with all electrons correlated.[35] Because of the computational cost, the largest basis set used was 6-31++G(d,p)[29] containing 298 basis functions, including a set of diffuse functions on all atoms in addition to polarization functions; also, for comparison, the smaller 6-31G(d,p) and basis sets without polarization or diffuse functions on H atoms were tested.

The CPMD program was used to obtain constrained DFT minimized geometries for rotation around the ring–amide (C–N) bond in **2** and **6**. One C-C-N-C ring–amide torsional angle (ρ) was held approximately fixed by a Lagrangian constraint[30] at a particular angle,[36] while all other parameters were relaxed. An isolated box of size $10\times12\times12$ Å was used for **2** and for **6**. The constrained angle ρ was varied from 0 to 90° for **2** and from 0 to 360° for **6**. For the $\rho=90°$ structure of **2**, the amide group was initially set to be in the plane perpendicular to the benzene ring. The constrained structures in this work are compromises: all distortions were allowed but were explored locally, not globally. Details are given in the Supporting Information. Note that no zero-point energy (ZPE) corrections were made to the energies for the torsional curves, since the various geometries are constrained and hence are in fact not stationary points. Some recent work on methylamine[37] included ZPE corrections by halving the contributions of the two lowest frequencies and/or ignoring any contribution from imaginary frequencies. It would be interesting to test this approach in future work.

Acknowledgements

Thanks to Dr. Simone Raugei for helpful discussions. This research is funded by NIH BECON grant RO1-GM-65803. Computer time from NPACI is greatly appreciated.

[1] a) A. E. Barron, R. N. Zuckermann, *Curr. Opin. Chem. Biol.* **1999**, *3*, 681–687; b) V. Berl, M. Schmutz, M. J. Krische, R. G. Khoury, J.-M. Lehn, *Chem. Eur. J.* **2002**, *8*, 1227–1244; c) S. H. Gellman, *Acc. Chem. Res.* **1998**, *31*, 173–180; d) D. J. Hill, M. J. Mio, R. B. Prince, T. S. Hughes, J. S. Moore, *Chem. Rev.* **2001**, *101*, 3893–4011; e) K. D. Stigers, M. J. Soth, J. S. Nowick, *Curr. Opin. Chem. Biol.* **1999**, *3*, 714–723; f) I. Huc, *Eur. J. Org. Chem.* **2004**, 17–29.

[2] a) J. S. Nowick, D. L. Holmes, G. Mackin, G. Noronha, A. J. Shaka, E. M. Smith, *J. Am. Chem. Soc.* **1996**, *118*, 2764–2765; b) J. S. Nowick, M. Pairish, I. Q. Lee, D. L. Holmes, J. W. Ziller, *J. Am. Chem. Soc.* **1997**, *119*, 5413–5424; c) H. Q. Zeng, R. S. Miller, R. A. Flowers, B. Gong, *J. Am. Chem. Soc.* **2000**, *122*, 2635–2644; d) J. Zhu, R. D. Parra, H. Zeng, E. Skrzypczak-Jankun, X. C. Zeng, B. Gong, *J. Am. Chem. Soc.* **2000**, *122*, 4219–4220; e) J. T. Ernst, J. Becceril, H. S. Park, H. Yin, A. D. Hamilton, *Angew. Chem.* **2003**, *115*, 553–557; *Angew. Chem. Int. Ed.* **2003**, *42*, 535–539; f) B. Gong, Y. Yan, H. Zeng, E. Skrzypczak-Jankunn, Y. W. Kim, J. Zhu, H. Ickes, *J. Am. Chem. Soc.* **1999**, *121*, 5607–5608.

[3] G. N. Tew, D. H. Liu, B. Chen, R. J. Doerksen, J. Kaplan, P. J. Carroll, M. L. Klein, W. F. DeGrado, *Proc. Natl. Acad. Sci. USA* **2002**, *99*, 5110.

[4] D. Liu, S. Choi, B. Chen, R. J. Doerksen, D. J. Clements, J. D. Winkler, M. L. Klein, W. F. DeGrado, *Angew. Chem.* **2004**, *116*, 1178–1182; *Angew. Chem. Int. Ed.* **2004**, *43*, 1158–1162.

[5] a) M. Zasloff, *Trends Pharmacol. Sci.* **2000**, *21*, 236–238; b) M. Zasloff, *Nature* **2002**, *415*, 389–395; c) H. G. Boman, *Immunol. Rev.* **2000**, *173*, 5–16; d) R. E. W. Hancock, R. Lehrer, *Trends Biotechnol.* **1998**, *16*, 82–88; e) J. A. Patch, A. E. Barron, *Curr. Opin. Chem. Biol.* **2002**, *6*, 872–877.

[6] R. J. Doerksen et al., unpublished results.

[7] a) A. B. Smith, III, L. Ducry, R. M. Corbett, R. Hirschmann, *Org. Lett.* **2000**, *2*, 3887–3890; b) S. Rajesh, J. Srivastava, B. Bannerji, J. Iqbal, *ARKIVOC* **2001**, *viii*, 20–26; c) S. J. Miller, H. E. Blackwell, R. H. Grubbs, *J. Am. Chem. Soc.* **1996**, *118*, 9606–9614; d) R. Nomura, J. Tabei, T. Masuda, *J. Am. Chem. Soc.* **2001**, *123*, 8430–8431.

[8] S. W. Johnson, J. Eckert, M. Barthes, R. K. McMullan, M. Muller, *J. Phys. Chem.* **1995**, *99*, 16253–16290.

[9] V. P. Manea, K. J. Wilson, J. R. Cable, *J. Am. Chem. Soc.* **1997**, *119*, 2033–2039.

[10] S. Ullrich, K. Müller-Dethlefs, *J. Phys. Chem. A* **2002**, *106*, 9181–9187.

[11] W. Caminati, A. Maris, A. Millemaggi, *New J. Chem.* **2000**, *24*, 821–824.

[12] S. François, M.-M. Rohmer, M. Bénard, A. C. Moreland, T. B. Rauchfuss, *J. Am. Chem. Soc.* **2000**, *122*, 12743–12750.

[13] a) N. Ueyama, K. Taniuchi, T. Okamura, A. Nakamura, H. Maeda, S. Emura, *Inorg. Chem.* **1996**, *35*, 1945–1951; b) T. Okamura, S. Takamizawa, N. Ueyama, A. Nakamura, *Inorg. Chem.* **1998**, *37*, 18–28.

[14] N. Ueyama, T. Okamura, Y. Yamada, A. Nakamura, *J. Org. Chem.* **1995**, *60*, 4893–4899.

[15] A. P. Scott, L. Radom, *J. Phys. Chem.* **1996**, *100*, 16502–16513.

[16] M. D. Halls, J. Velkovski, H. B. Schlegel, *Theor. Chem. Acc.* **2001**, *105*, 413–421.

[17] R. J. Doerksen, B. Chen, M. L. Klein, *Chem. Phys. Lett.* **2003**, *380*, 150–157.

[18] T. Steiner, *Angew. Chem.* **2002**, *114*, 50–80; *Angew. Chem. Int. Ed.* **2002**, *41*, 48–76. Note that Steiner defines "weak" hydrogen bonds as an extension of the definition of regular hydrogen bonds by several criteria, including allowing dissociation energies less than 4 kcal mol^{-1}, angles as low as 90°, an IR X–H stretching red shift of less than 10%, and X–H lengthening by less than 0.02 Å.

[19] a) G. A. Jeffrey, *An Introduction to Hydrogen Bonding*, Oxford University Press, Oxford, **1997**; b) S. Scheiner, *Hydrogen Bonding. A*

 © 2004 Wiley-VCH Verlag GmbH & Co. KGaA, Weinheim

Theoretical Perspective, Oxford University Press, Oxford, **1997**; c) G. R. Desiraju, T. Steiner, *The Weak Hydrogen Bond in Structural Chemistry and Biology*, Oxford University Press, Oxford, **1999**.

[20] a) A. Rahman, D. van der Helm, *Acta Crystallogr. Sect. B* **1980**, *36*, 2444–2447; b) F. H. Allen, C. M. Bird, R. S. Rowland, P. R. Raithby, *Acta Crystallogr. Sect. B* **1997**, *53*, 696–701, from the Cambridge Structural Database up to 1995. c) T. Steiner, *J. Phys. Chem. A* **1998**, *102*, 7041–7052. d) F. Hdii, J.-P. Reboul, J. Barbe, D. Siri, G. Pepe, *Acta Crystallogr. Sect. C* **1998**, *54*, 391–392.

[21] Y. Gu, T. Kar, S. Scheiner, *J. Am. Chem. Soc.* **1999**, *121*, 9411–9422.

[22] a) G. R. Desiraju, *Acc. Chem. Res.* **2002**, *35*, 565–573; b) R. Vargas, J. Garza, D. A. Dixon, B. P. Hay, *J. Am. Chem. Soc.* **2000**, *122*, 4750–4755; c) F. M. Raymo, M. D. Bartberger, K. N. Houk, J. F. Stoddart, *J. Am. Chem. Soc.* **2001**, *123*, 9264–9267; d) P. W. Baures, A. M. Beatty, M. Dhanasekaran, B. A. Helfrich, W. Pérez-Segarra, J. Desper, *J. Am. Chem. Soc.* **2002**, *124*, 11315–11323; e) A. Donati, S. Ristori, C. Bonechi, L. Panza, G. Martini, C. Rossi, *J. Am. Chem. Soc.* **2002**, *124*, 8778–8779; f) L. Jiang, L. Lai, *J. Biol. Chem.* **2002**, *277*, 37732–37740; g) I. V. Alabugin, M. Manoharan, S. Peabody, F. Weinhold, *J. Am. Chem. Soc.* **2003**, *125*, 5973–5987.

[23] a) S. Glasstone, *Trans. Faraday Soc.* **1937**, *33*, 200; b) C. G. Pimental, A. L. McClellan, *The Hydrogen Bond*, W. H. Freeman, San Francisco, **1960**, pp. 197–201; c) A. Allerhand, P. von R. Schleyer, *J. Am. Chem. Soc.* **1963**, *85*, 1715–1723; d) D. J. Sutor, *J. Chem. Soc.* **1963**, 1105–1110.

[24] If one considers rotating ρ from 0 to 180°, however, symmetry will cause the C2–H curve in Figure 4 to overlap the C6–H curve. Therefore, in Figure 4 the two sets of data for **2** are plotted as though they represent only either C2–H or C6–H for $\rho = 0$ to 180°.

[25] Gaussian 98 (x86-Linux-G99; Revision A.3), M. J. Frisch, G. W. Trucks, H. B. Schlegel, G. E. Scuseria, M. A. Robb, J. R. Cheeseman, V. G. Zakrzewski, J. A. Montgomery, Jr., R. E. Stratmann, J. C. Burant, S. Dapprich, J. M. Millam, A. D. Daniels, K. N. Kudin, M. C. Strain, O. Farkas, J. Tomasi, V. Barone, M. Cossi, R. Cammi, B. Mennucci, C. Pomelli, C. Adamo, S. Clifford, J. Ochterski, G. A. Petersson, P. Y. Ayala, Q. Cui, K. Morokuma, D. K. Malick, A. D. Rabuck, K. Raghavachari, J. B. Foresman, J. Cioslowski, J. V. Ortiz, A. G. Baboul, B. B. Stefanov, G. Liu, A. Liashenko, P. Piskorz, I. Komaromi, R. Gomperts, R. L. Martin, D. J. Fox, T. Keith, M. A. Al-Laham, C. Y. Peng, A. Nanayakkara, C. Gonzalez, M. Challacombe, P. M. W. Gill, B. G. Johnson, W. Chen, M. W. Wong, J. L. Andres, M. Head-Gordon, E. S. Replogle, J. A. Pople, Gaussian, Inc., Pittsburgh PA, **1999**.

[26] a) W. Kohn, A. D. Becke, R. G. Parr, *J. Phys. Chem.* **1996**, *100*, 12974–12980; b) M. Head-Gordon, *J. Phys. Chem.* **1996**, *100*, 13213–13225.

[27] a) A. D. Becke, *Phys. Rev. A* **1988**, *38*, 3098–3100; b) C. Lee, W. Yang, R. G. Parr, *Phys. Rev. B* **1988**, *37*, 785–789.

[28] A. D. Becke, *J. Chem. Phys.* **1993**, *98*, 5648–5652; b) S. H. Vosko, L. Wilk, M. Nusair, *Can. J. Phys.* **1980**, *58*, 1200–1211; c) P. J. Stephens, F. J. Devlin, C. F. Chabalowski, M. J. Frisch, *J. Phys. Chem.* **1994**, *98*, 11623–11627.

[29] D. Feller, E. R. Davidson in *Reviews in Computational Chemistry*, *Vol. 1*(Eds.: K. B. Lipkowitz, D. B. Boyd), VCH, New York, **1990**, pp. 1–43.

[30] a) R. Car, M. Parrinello, *Phys. Rev. Lett.* **1985**, *55*, 2471–2474; b) J. Hutter, A. Alavi, T. Deutsch, M. Bernasconi, S. Goedecker, M. Tuckerman, M. Parrinello, CPMD version 3.4, MPI für Festkörperforschung and IBM Research Laboratory, Stuttgart and Zürich, **1995–2000**.

[31] D. Marx, J. Hutter, *Ab Initio Molecular Dynamics: Theory and Implementation* in *Modern Methods and Algorithms of Quantum Chemistry* (Ed.: J. Grotendorst), *NIC Series*, **2000**, *Vol. 1*, NIC-Directors, FZ Jülich.

[32] F. A. Hamprecht, A. J. Cohen, D. J. Tozer, N. C. Handy, *J. Chem. Phys.* **1998**, *109*, 6264–6271.

[33] N. Troullier, J. L. Martins, *Phys. Rev. B* **1991**, *43*, 1993–2006.

[34] L. Kleinman, D. M. Bylander, *Phys. Rev. Lett.* **1982**, *48*, 1425–1428.

[35] W. J. Hehre, L. Radom, P. von R. Schleyer, J. A. Pople, *Ab Initio Molecular Orbital Theory*, Wiley, New York, **1986**.

[36] Note that if the constrained angle was set close to planar (either 0 or 180°), then it tended to wander away from that constrained value by several degrees because of the way the dihedral angle constraint is implemented in the CPMD program; other values of the angle could be constrained to within 0.1°.

[37] Y. G. Smeyers, M. Villa, *Chem. Phys. Lett.* **2000**, *324*, 273–278.

Received: February 23, 2004
Published online: August 30, 2004

 © 2004 Wiley-VCH Verlag GmbH & Co. KGaA, Weinheim